Optical limiting and nonlinear optical properties of Cr2O3 and WO3 based polymer nanocomposites

O. Muller, M. Guerchoux, Pierre Gibot, L. Merlat, D. Spitzer

Optical limiting and nonlinear optical properties of Cr_2O_3 and WO_3 based polymer nanocomposites

O. MULLER*[1], M. GUERCHOUX[1], P. GIBOT[2], L. MERLAT[1] AND D. SPITZER[2]

[1]*Laboratory for Radiation Interaction with Matter, French-German Research Insitute of Saint-Louis (ISL), 5 rue du Général Cassagnou, 68301 Saint-Louis, France*
[2] *Laboratoire des Nanomatériaux pour Systèmes Sous Sollicitations Extrêmes (NS3E), CNRS/ISL/UNISTRA UMR 3208, French-German Research Insitute of Saint-Louis (ISL), 5 rue du Général Cassagnou, 68301 Saint-Louis, France*
** Corresponding author: olivier.muller@isl.eu; phone +33 3 89 69 58 59; www.isl.eu*

Abstract: The coming decades will be the scene of a massive deployment of laser systems both in civil society and for military purposes. Emerging new technologies have to face strong challenges on their ability to become more efficient and faster in response time. Whilst nothing can travel faster than the speed of light, photons technologies like lasers might become ubiquitous and swarms of lasers emitting harmful radiations will become the center of a growing interest. At the other end of the segment, the complementary activity is to enable for efficient, tough versatile protection methods toward the laser weaponry. Nonlinear optical nanomaterials can serve this purpose when properly embedded in a solid medium, resulting in nanocomposite passive optical limiting filters. The present study relies on the passive laser protection concept where materials with nonlinear optical properties are used, that are self-activated when the incident laser threat is above a certain level of intensity. Nanomaterials are tailored for optical limitation due to their versatility, their strong nonlinear absorption properties and their uniform transmittance characteristics over a broad spectral range, the latter property avoiding color distortions to the observation device. The optical limiting behavior of templated transition metals nanoparticles, Cr_2O_3 and WO_3 in a PMMA host at the wavelength of 1064 nm in the nanosecond regime is discussed. The optical filter were produced by chemical synthesis from the bulk. The optical limiting properties were characterized using an adequate custom-made optical setup and the third order nonlinear parameters, namely the nonlinear absorption coefficients and refractive indices were measured by the Z-scan method. The optical limiting performance improvement is clearly demonstrated for the PMMA/Cr_2O_3 filter bearing out a laser protection level of OD=2.0, a factor of 2 larger than the pure PMMA filter. A significant blue shift in the nonlinear activation threshold energy occurs when WO_3 or Cr_2O_3 are embedded in a PMMA host as the values have been subsequently pulled down from 500 µJ (pure PMMA) to 65 µJ and 23µJ, respectively. Z-scan measurements highlighted a self-defocusing effect as a result of a negative nonlinearity. Nonlinear refractive indexes in the order of $n_2 = -1.0\,X\,10^{-15}\,cm^2/W$ were calculated for the PMMA/Cr_2O_3 and PMMA/ WO_3 systems and $n_2 = -2.2\,X\,10^{-17}\,cm^2/W$ for the pure PMMA. A nonlinear absorption coefficient as high as $\beta = 163\,cm/GW$ was measured for the PMMA/Cr_2O_3 optical limiting filter while the one for the pure PMMA lies 2 orders of magnitude behind. It is suggested that the PMMA/Cr_2O_3 optical system undergoes reverse saturable absorption enhanced by excited state absorption (ESA/RSA). Besides, it is believed that multi-photons absorption (MPA) occurs in PMMA/WO_3 or pure PMMA.

1. Introduction

Recent advances in laser technology and the miniaturization of optical devices have ushered in a new era of efficiency for the military as well as for the civilian laser systems. Visible and IR light receptors are capable of detecting electromagnetic radiation at various intensity levels and at various wavelengths in the spectral region from approximately 400 nm to 5000 nm. Examples of such light receptors include but are not limited to the human eye and optical detectors/sensors which produce a response whenever illuminated. The human eye, optical detectors/sensors and photo-receptors can be damaged by exposure to high intensity lasers. For example, optical detectors can be exposed beyond their capabilities and destroyed by either continuous or short duration exposure to a laser beam. Similarly, the retina of the eye can be damaged by being exposed to a laser beam for only a brief period of time.

The objective of this work is to synthesize nonlinear optical polymer nanocomposite filters based on Cr_2O_3 and WO_3 bearing out optical limiting properties. The use of nonlinear optical materials offers the possibility to design passive protection filters, i.e., those activated by the incoming radiation itself, in contrast to active systems, trickier in their elaboration, where the input signal has to be controlled by an additional element [1]. Obviously speaking, an optical limiting filter must fulfill the following conditions: possess a fast response time, exhibit a low nonlinear threshold, be neutral in color, present a low insertion loss (i.e., a high linear transmittance) and cover a large spectral range. Poly(methyl methacrylate) (PMMA) is considered as the host material in this study.

Solid-state optical limiting nanocomposite filters consist frequently of PMMA as the host material, which is a widely used polymeric material in the fields of defense and aerospace as well as in the field of laser protection, see e.g. [2-5]. PMMA is the most common organic glass, it exhibits excellent properties such as small chromatic dispersion, high linear transmittance in the VIS, NIR and the SWIR part of the spectrum. Metal oxide nanomaterials formed from transition metals like Cr_2O_3 and WO_3 are known to be p-type and n-type semiconductors, respectively. Chromium and tungsten, referred in the group 6B elements have interesting electronic band structures ruling out their chemical and physical properties. Actually, they form partially filled d-orbitals which will extend up to the conduction band and even exceed the Fermi level, so they present a complete overlap of the conduction band by the valence band. Accordingly, interband electronic transitions can be readily assumed in the VIS up to the NIR part of the electromagnetic spectrum in the case of Cr_2O_3 and WO_3. Furthermore, these appropriate interband transitions will promote (nonlinear) absorption effects and contribute to the dielectric function of the materials which outlines the manner the electromagnetic radiations act on the electrons involved. Regarding their promising electronic properties, Cr_2O_3 and WO_3 should be reasonably considered as good candidates for optical limiting applications where nonlinear absorption effects are the basic prerequisites. Although the research studies relating on the electronic and optical properties of Cr_2O_3 and WO_3 [6-9] (among others), and those reporting on their optical limiting behavior [10-20] are numerous, to the best of the authors knowledge there is no work describing the nonlinear optical properties as well as the optical limiting behavior of nanocomposites made of Cr_2O_3 and WO_3 nanofillers embedded in a PMMA matrix.

This work focuses on the nonlinear optical effects resulting from pulsed laser radiations in the near infrared at the wavelength of 1064 nm at the nanosecond timescale. Actually, harmful radiations are often due to laser target designators emitting invisible beams (to the eyes) at the wavelength of 1064 nm [21,22]. In section 2 we expose the experimental principles of this work. In section 3, resulting from nonlinear transmittance measurements, the filters performance are given in terms of their global nonlinear attenuation. In a further step, by means of Z-scan assessments we study the nonlinear absorption and the nonlinear refraction of the optical limiters. Section 4 gives the conclusion of this work.

2. Experimental section

2.1 Chemical synthesis

Templated Cr_2O_3 and WO_3 nanoparticles were synthesized following the procedure described in [20, 23, 24]. Succinctly, the synthesis of chromium (III) oxide and tungsten(VI) oxide nanoparticles were carried out as follow: metal salts (Cr, W) were dissolved in an aqueous dispersion of nanosized SiO2 particles (Ludox®) according to a silica/metal precursor weight ratio of 2/3.The resulting mixtures were stirred for 1 h to achieve homogeneous suspensions, placed in an oven at 80 °C to obtain total evaporation of the aqueous phase and then grounded in a mortar. The powdered samples were calcinated 2 h at a heating rate of 2 °C/min at 550 °C and 600 °C for the Cr-based and W-based composites, respectively. The pristine Cr- and W-based composites were washed twice with hydrofluoric acid (10 wt%) to remove the silica nanoparticles. The ceramic materials were separated to the acid phase via centrifugation and washed with distilled water then once with acetone. Finally, the green (Cr) and yellow (W) oxide materials were dried in an oven at 100 °C overnight. Methyl methacrylate (MMA) monomer (5 mL, 4.7 g, purchased from Carl Roth) and the composites nanoparticles were mixed in 20 mL welted glass. The same mass fraction was used for Cr_2O_3 and WO_3: mother solutions with a nanoparticle load of 0.025 wt% were prepared and subsequently diluted to obtain the final mass fraction of 0.0025 wt%. Both resulting solutions were mixed in an ultrasonic bath during 10 min. A micro-magnetic bar was added to homogenize the solutions during the reaction. Then, the AIBN initiator was added at 0.4wt%. To efficiently disperse the AIBN, a Vortexer was used during 1 min. In a further step, septum was used to keep closed mixtures during the reaction. These latter were put in an ice bath to avoid the MMA monomer from evaporating before it was degased with nitrogen for one minute. During the process the solutions were surmounted with a nitrogen bag. Mixtures were then heated up, maintained at 50 °C in an oil bath and simultaneously stirred. When solutions appeared to be too viscous, the micro-magnetic bar was removed and the welted glass was put in an oven at 50°C until a solid bulk was obtained. The glass was opened to allow the unreacted MMA monomer (mainly located in the top layer above the polymer) to escape. Finally, the welted glass was broken and separated from the solid polymer before it was polished to obtain optical-grade quality filters. The 2.5 mm thick resulting laser protection filters are shown on figure 1.

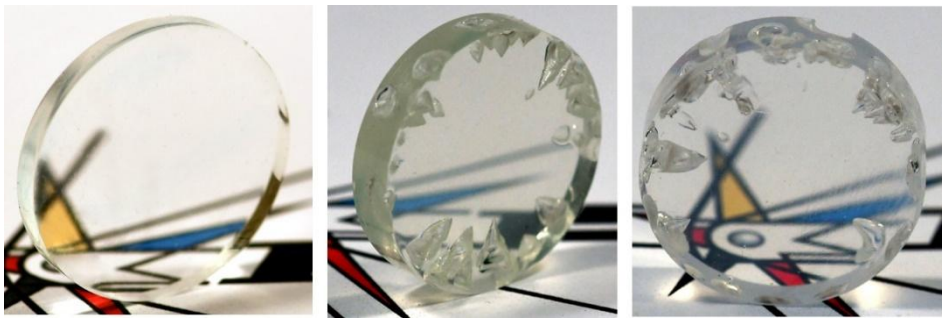

Fig. 1: Optical limiting filters, from the left to the right respectively, pure PMMA, PMMA/Cr_2O_3 and PMMA/WO_3. Both pictures on the right highlight the Trommsdorff effect.

Featured on both photographs on the right of figure 1, the conical texture observed on the periphery of the optical filters is due to the Trommsdorff effect [25], often occurring in free radical bulk polymerizations. In brief, the Trommsdorff effect is a side reaction leading to a dramatic reduction of the termination reaction rates due to the diffusion limitation and the local rise in viscosity of the polymerizing arrangement. As a consequence of the lack of

reaction obstacles, the polymerization rate is significantly increased, therefore leading in uncontrollable reactions.

2.2 Linear optical properties

The linear transmittance of the optical filters as well as their linear absorbance are shown on figures 2 and 3, respectively. The measurements were carried out by using a double beam UV/VIS/SWIR spectrometer Agilent Cary 7000 in the wavelength range [250 nm-1100 nm] and [220 nm-600 nm], respectively. It is obvious to mention that the presence of Cr_2O_3 and WO_3 nanoparticles significantly affect the linear optical properties of PMMA as it can be seen on the figures 2 & 3. Nevertheless, in the wavelength range of interest, the linear transmittance of the optical filters can be considered as broadband and the value of T=90 % at 1064 nm meets the specifications for an optical limiting filter.

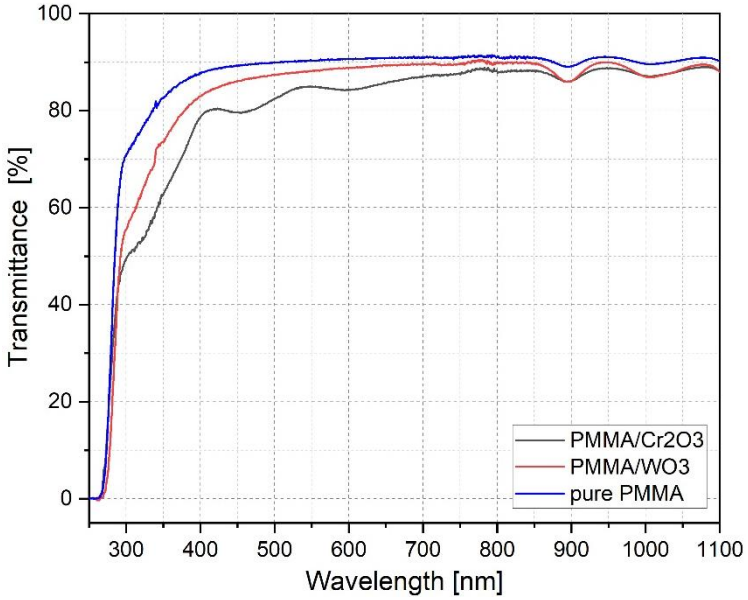

Fig. 2: Linear transmittance spectra of PMMA/Cr_2O_3 and PMMA/WO_3 optical limiting filters. Comparison with pure PMMA.

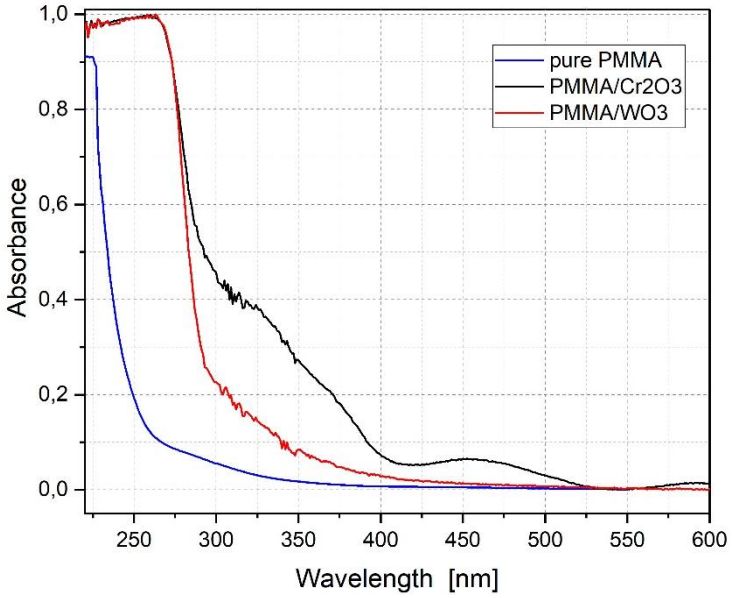

Figure 3: Absorption spectra of PMMA/Cr_2O_3 and PMMA/WO_3 optical limiting filters. Comparison with pure PMMA.

As it is revealed on figures 2 & 3, the PMMA/Cr_2O_3 filter shows a strong absorption in the violet around 350 nm in accordance with the greenish color of the optical filter. It is well known that the optical properties of Cr^{3+} ions in Cr_2O_3 are due to d-d electronic transitions. Actually, 2 well defined bands can be observed at 460 nm and 600 nm in agreement with the work of Liang et al. [26]. These bands may be assigned to the $^4A_{2g} \rightarrow {}^4T_{1g}$ transitions of the six coordinate geometry and the $^4A_{2g} \rightarrow {}^4T_{2g}$ of Cr^{3+} ions in an octahedral environment [26]. On the other hand, the PMMA/WO_3 system exhibits quasi-monotonic transmittance and absorbance behaviors which might be related to the symmetrical nature of tungsten trioxide monoclinic crystal lattice structure and the absence of specific intragap defects. The well resolved sharp edge between 300 nm and 400 nm is to be imparted to the presence of oxygen ions vacancies in the structure of WO_3 [27]. The slight bluish color of the PMMA/WO_3 filter (figure 1) is due to gap narrowing as a consequence of these O vacancies.

Investigations on the intrinsic absorption edge of the optical limiting filters in figure 3 enable to determine the optical band gap of the materials according to the absorption spectrum fitting method using the Tauc model well described in [28]. Taking into account indirect band to band transitions, the Tauc plot, i.e. the plot $(Absorbance \quad / \lambda)^{1/m}$ versus $1/\lambda$ is expected to show a linear behavior in the high energy region which corresponds to a strong absorption near the absorption edge. By extrapolating the linear portion of this straight line to zero absorption edge provides the optical energy band gap, Eg of the polymer based optical filters. It is observed that the best fitting procedure is obtained for $m = 2$, therefore consistent with allowed indirect $\pi^* - \pi$ electronic transitions in material structures for which the top of the valence band is not at the same wave vector point as the bottom of the conduction band. The value of Eg is easily deduced by multiplying the extrapolated abscissa by 1239.83 (the combination of the Planck's constant and the velocity of light). The results can be seen on the figure 4 and the Eg values are summarized in table 1.

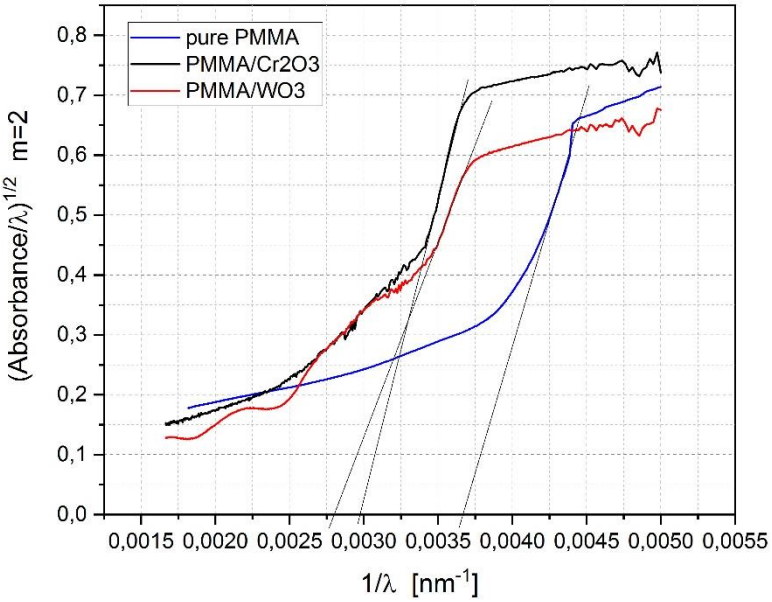

Figure 4: Assessment of the optical band gaps. Tauc plots for PMMA/Cr_2O_3, PMMA/WO_3 and pure PMMA optical limiting filters.

Table 1: Optical band gaps for PMMA based optical limiting filters.

	pure PMMA	PMMA/Cr_2O_3	PMMA/WO_3
E_g (eV)	4.6	3.7	3.5

It appears noteworthy that pure PMMA exhibits the highest Eg value of 4.6 eV in consistency with its insulator character. Our experimental value is in accordance with the one determined by Jasim et al., Eg=4.6 eV [29], and the one obtained in [30], Eg=4.9 eV. Our experimental findings on figure 4 and table 1 indicate that the optical band gap of pure PMMA is decreased due to the presence of semiconducting nanoparticles like Cr_2O_3 and WO_3. All synthesized nanocomposites were characterized by a lower optical energy gap Eg than the matrix polymer material as already observed by Matysiak et al. [31]. Indeed, energy band gaps of 3.7 eV and 3.5 eV stem from our experimental work in the case of PMMA/Cr_2O_3 and PMMA/WO_3, respectively. To the best appreciation of the authors, there is a strict lack of Eg data in the literature for PMMA nanocomposites made of Cr_2O_3 or WO_3 loads. Albeit our values cannot be strictly compared to pure compounds, Abdullah et al. calculated a value Eg=3.2 eV for as-grown Cr_2O_3 nanostructures [32], whereas regarding WO_3 thin films, Sivakumar et al. obtained Eg values ranging from 2.7 eV to 3.1 eV [27], both of which are in harmony with our findings.

2.3 Optical setup and measurement procedure

The laser system used for this study is a Q-switched Nd-YAG (Quantel) working at the wavelength of 1064 nm with a repetition rate fixed to 1 Hz and a pulse width of nearly 4 ns. The experimental setup to assess the nonlinear transmittance is sketched in figure 5 and the detailed experimental process is given in [1].

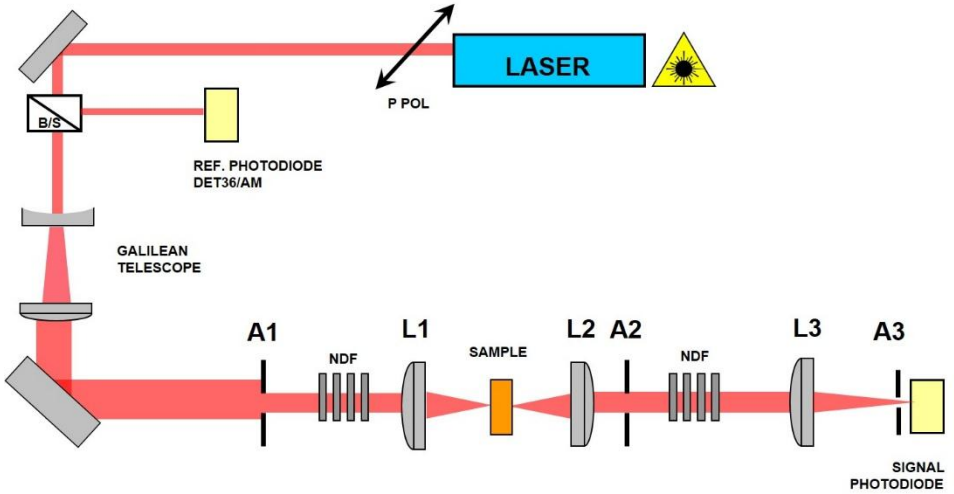

Fig. 5: Experimental setup used to study the optical limiting behavior of nonlinear filters. Details on the setup given in [1].

One part of the incident laser beam is taken from the main setup right before the Keplerian telescope (see figure 5) and directed toward the Z-scan experimental setup shown in figure 6. Precise informations on the measurement procedure can be read in [1].

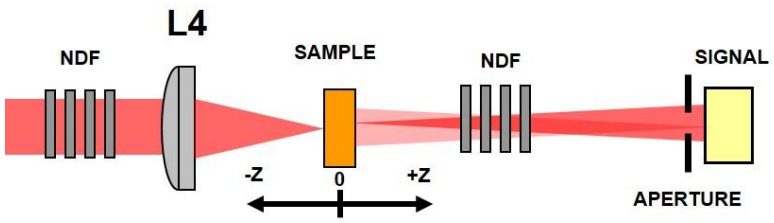

Fig. 6: From [1]. Z-scan optical setup in an open and close aperture scheme. L_4, plano-convex lens, f_4 = 200 mm; NDF, neutral density filters; aperture hole, 200 µm.

3. Results and discussion

3.1 Nonlinear optical transmittance

The assessment of the transmittance as a function of the laser incident energy, in off-resonant conditions (i.e., 1064 nm), reveals the co-existence of 2 regimes governed by a linear behavior and a nonlinear one, respectively. The experimental results depicted in figure 7 at the wavelength of λ=1064 nm are supported by theoretical fitting sessions displayed in solid lines. The laser input energy was varied from 1 nJ up to ca. 4 mJ. The linear regime, where the transmittance is constant, spreads over several decades of input energies is followed by the nonlinear regime characterized by a decrease of the optical filters transmittance. It is to be noticed that the height of the plateau giving the transmittance of each filter at 1064 nm is in good agreement with the spectrometer transmittances given in figure 2. The optical limiting threshold, is a crucial parameter since it describes the efficiency of each optical limiting filter and is defined as the energy where the transmittance drops to 3 dB of its initial value. This parameter is obtained by a direct lecture on the graphs of figure 7 and should be appropriately compared with the energy thresholds resulting from theoretical fitting whose depending on

more complex constraints. Readily, those are 23 µJ, 65 µJ and 500 µJ for the PMMA/Cr_2O_3, PMMA/WO_3 and pure PMMA, respectively.

Obviously, PMMA/Cr_2O_3 optical filter shows the most favorable optical limiting performance. Indeed, it presents the sharpest decrease of the transmittance, as high as 8 dB per decade compared to a steepness of 3 dB per decade for PMMA/WO_3 optical filter. As expected, the worse achievement concerns the pure PMMA optical filter. At the highest incident energy, a direct lecture on figure 7 brings the global filters attenuation to be OD=2.0, OD=1.0 and OD=0.9, for the PMMA/Cr_2O_3, PMMA/WO_3 and pure PMMA, respectively.

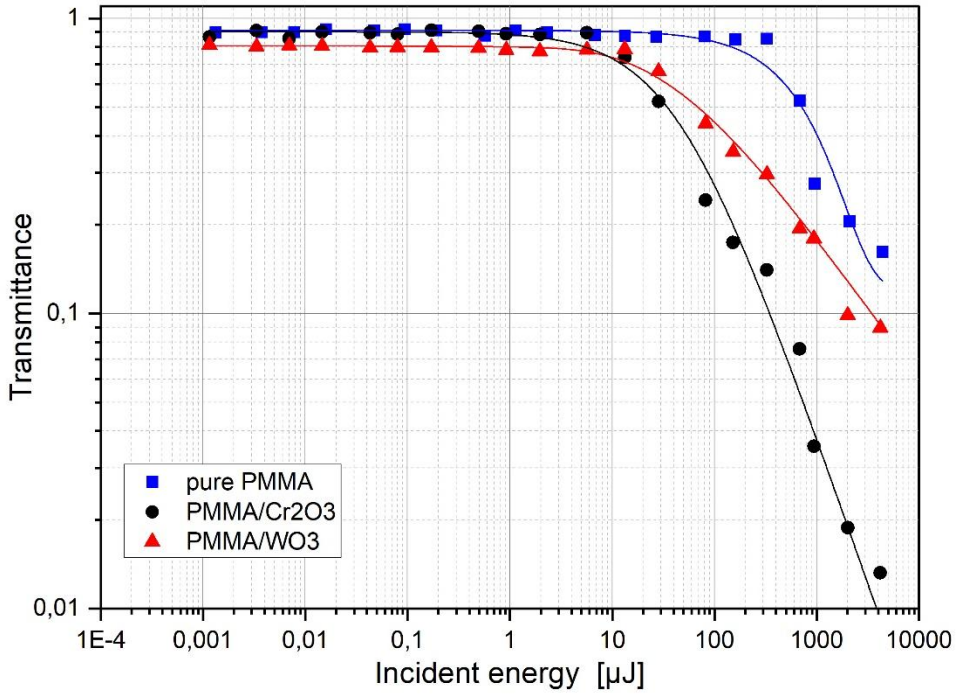

Fig. 7: Transmittance as a function of the input energy displayed in a log–log plot for the 3 filter systems under investigation. Solid lines result from theoretical fitting. Laser wavelength is 1064 nm. Further details are mentioned in the text.

It is firmly to be expected that molecular arrangements involving transition metals, like e.g., Cr in the case of PMMA/Cr_2O_3, undergo excited state absorption / reverse saturable absorption (ESA/RSA) at an appropriate laser energy level. Experimental findings in several research studies tend to confirm our statement [5, 33-35]. In [5], Liao et al. demonstrated that the incorporation of MoS_2 nanostructures in a PMMA host offered incentives to promote RSA as the nonlinear optical limiting behavior. Varma et al. in their research article [33], described a superior optical limiting material based on Ti, another transition metal and ascribed the nonlinear effects to multi-photons and the induced excited state absorptions. Also, Sharma et al. [34, 35] investigating hybrid nanostructures of $NiCo_2O_4$ observed that their nonlinear behavior was mediated by ESA/RSA. It is likely that ESA/RSA in PMMA/Cr_2O_3 occurs in a 2 steps process: first, interband transitions from the valence band into the low spin state conduction band and second, intraband transitions within the conduction band. Basically, in the case of Cr_2O_3, the valence band is mainly composed of Cr 3d and O 2p states, whereas the bottom of the conduction band is filled by Cr 3d states [36].

Hence, the photoinduced electrons may hope from the valence into the conduction band between the O 2p orbitals and the Cr 3d orbitals.

To verify the aforementioned claims, the transmission was numerically solved by using a theoretical model based on ESA/RSA. Briefly speaking, this model assumes that the absorption cross section is a function of the laser energy density E travelling (along z) through a nonlinear absorptive medium which can be written as:

$$dE / dz = -\sigma E N_0 - \mu_1 E^2 N_0 \qquad (1)$$

Where σ_0 denotes the ground state absorption cross section, μ_1 is the absorption cross section of the first excited singlet state and N_0 is the density of state. $\sigma_0 N_0$ and $\mu_1 N_0$ are the linear and nonlinear absorption coefficients, respectively.

Equation (1) can be easily integrated and one obtains,

$$E_{out} = T_0 E_{in} / [1 + (1 - T_0) E_{in} / E_{th}] \qquad (2)$$

In relation (2), E_{in}, E_{out} and E_{th} represent the input, output and threshold energy or energy density, respectively. T_0 is the linear transmittance.

The equation in relation (2) assuming ESA / RSA phenomena in the molecular medium has been used for theoretical fittings of the transmittance dependence on the laser input energy of figure 7.

The theory explaining the nonlinear optical limiting phenomena in PMMA/WO_3 or pure PMMA is somewhat different and we believe it originate from multi-photons absorption mechanisms (MPA). By virtue of the formalism described as given example in [37], the transmittance T as a function of the input energy or energy density is given by relation (3),

$$T = T_0 \left[C.\exp\left\{ -\left(\frac{Ein}{Eth} \right)^{1/2} \right\} + (1 - C)(1 - \exp\left\{ -\left(\frac{Ein}{Eth} \right)^{-1/2} \right\}) \right] \qquad (3)$$

In (3), C designates a constant related to the nonlinear attenuation of the materials (not necessarily pure nonlinear absorption). As shown on the line plots of figure 7, it is very interesting to notice that the MPA formalism well fits with the experimental data for PMMA/WO_3 or pure PMMA. Furthermore, equations (2) and (3) allow to estimate the threshold energy E_{th}, as it is considered as a fitting parameter. Results are shown below in the table 2. It is worth noting that the experimental and theoretical nonlinear thresholds for optical limiting behave in the same order of magnitude except in the case of PMMA/Cr_2O_3 optical limiting filter.

Table 2: Optical limiting thresholds data. Experimental assessment by a lecture on figure 7 and results from theoretical modeling.

Optical Limiting thresholds (µJ)	Experimental	Theoretical Fitting
PMMA/Cr_2O_3	23	4
PMMA/WO_3	65	72

pure PMMA	500	490

3.2 Nonlinear absorption and nonlinear refraction

Nonlinear absorption and nonlinear refraction in optical materials can be both quantified using the Z-scan technique which is a sensitive and reliable characterization method. This technique is meticulously described in the work of Sheik-Bahae et al. [37]. In order to investigate the nonlinear refraction in our samples, the Z-scan in its closed aperture scheme presented on figure 6 was used. Open Z-scan transmittance measurements hinting at the nonlinear absorption coefficients were also performed. The sensitivity of the measurement depends on the aperture factor S which has to be carefully defined. The appropriate value of S in our investigations is S = 2 %. The close Z-scan experimental traces of the PMMA/Cr_2O_3 and PMMA/WO_3 optical limiting filters were produced at an irradiance level of $I_0 = 5.10^{10} W/cm^2$ ($E_{in} = 100\ \mu J$) and $I_0 = 5.10^{11} W/cm^2$ ($E_{in} = 1mJ$) for the pure PMMA filter. The reason for this discrepancy is blindingly obvious since a Z-scan experiment has to be related to the nonlinear behavior of the material. The nonlinear transmittance assessments of figure 7 is essential since it helps to find the dichotomy between the linear and the nonlinear regime. Moreover, we carefully controlled the absence of laser damage in the filters at those irradiances (energies). Experimental and theoretical fitting results are displayed on the figure 8. Basically, the trend observed for the close Z-scan experiments of figure 8 confirms the nonlinear behavior exposed in figure 7, thereby the most pronounced nonlinear effects occur in the PMMA/Cr_2O_3 system.

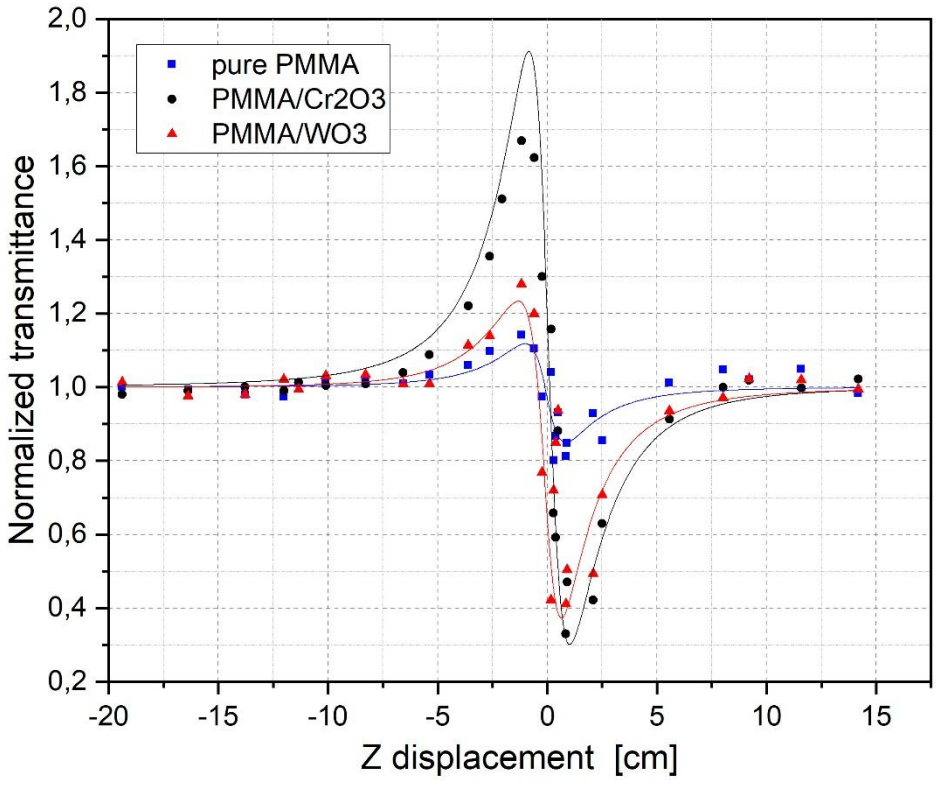

Figure 8: Close Z-scan results for the PMMA/Cr_2O_3 and PMMA/WO_3 optical limiting filters at an incident laser irradiance $I_0 = 5.10^{10} W/cm^2$ and pure PMMA at an incident laser irradiance $I_0 = 5.10^{11} W/cm^2$. The solid lines denote the theoretical fittings of equation (7). Laser wavelength is 1064 nm.

The theoretical fits on figure 8 result from the equations modeling the normalized transmittance when self-focusing or self-defocusing occur whereby the nonlinear refractive index, n_2 might be deducted. When a third order nonlinearity is accounted for, the refractive index n can be expressed as:

$$n = n_0 + n_2.I = n_0 + \Delta n \qquad (4),$$

where I denotes the peak irradiance, $I = I_0 = 5.10^{10} W/cm^2 or\ 5.10^{11} W/cm^2$ and n_0 the linear refraction coefficient.

The expression for the normalized transmittance, $T(z)$, in our case can be written as:

$$T(z) = 1 + \frac{4a}{(a^2+9)(a^2+1)}\Delta\Phi_0 - \frac{2(a^2+3)}{(a^2+9)(a^2+1)}\Delta\Psi_0 \qquad (5).$$

In relation (5), a denotes the reduced displacement and is expressed as $a = z/z_0$ (z is the linear displacement). $\Delta\Phi_0$ and $\Delta\Psi_0$ are major parameters that characterize the wave distortion and the subsequent phase shift around the focal point due to nonlinear refraction and nonlinear absorption, respectively. For both terms we can write:

$$\Delta\Phi_0 = kn_2 I_0 L_{eff} \qquad (6),$$

$$\Delta\Psi_0 = \beta I_0 L_{eff}/2 \qquad (7).$$

The observed peak to valley shapes of figure 8 indicate a self-defocusing effect as a result of a negative nonlinearity. Consequently, it is reasonable to argue for a thermally-induced n_2 refractive index change independently of the nature of the optical limiting filter.

From evidence, strong nonlinear refractive effects occur in the PMMA/Cr_2O_3 system, whereas it can be seen that the PMMA/WO_3 optical limiting filter exhibits an asymmetric shape like a reduced peak and a pronounced valley. This very interesting observation points the contribution of nonlinear absorption in accordance with the observations of Sheik-Bahae et al. in [37]. Actually, these authors demonstrated that nonlinear absorption like two-photon absorption (TPA) or multiphoton absorption suppresses the peak and enhances the valley in a close Z-scan scheme. The occurrence of TPA in PMMA/WO_3 is to be ruled out regarding its optical band gap, E_g = 3.5 eV, given in table 1. Yet, a MPA process like 3 photons absorption is more likely to occur at an incident photons energy of 1.1 eV (i.e., 1064 nm). As in the case of PMMA/Cr_2O_3, the close Z-scan findings for PMMA/WO_3 well match the estimated fittings of the nonlinear transmittance revealing MPA as the major nonlinear phenomenon. The n_2 values calculated owing to relations (5) and (6) are $n_2 = -1.6X10^{-15} cm^2/W$ for PMMA/Cr_2O_3, $n_2 = -7.1X10^{-16} cm^2/W$ for PMMA/ WO_3 and $n_2 = -2.2X10^{-17} cm^2/W$ for the pure PMMA (see also table 3).

The thermal nature of the nonlinearity originates from laser-induced heating subsequent to the absorption of the tightly focused laser beam. Accordingly, a strong temperature gradient occurs in conjunction with a severe refractive index change leading to a thermal lensing effect as well as a markedly phase distortion $\Delta\Phi_0$ of the propagating laser radiation. Such an effect may consist of a fast process of acoustic wave propagation and a slow steady state variation of the suspension density due to the cumulative thermal heating of the absorbing area.

It is likely that Cr_2O_3 and WO_3 nanofillers embedded in the PMMA host readily absorbs the incident laser radiations and reshuffle the energy in the surrounding medium in the form of heat. The refractive nonlinearity in PMMA/Cr_2O_3 might be connected with the cumulative contribution made by the processes of intraband transitions of free equilibrium electrons and nonlinear hyperpolarizability of bound 3d3 electrons. In a previous paper [20], the authors calculated nonlinear refractivity values $n_2 \approx 10^{-14}\, cm^2/W$ for Cr_2O_3 and WO_3 suspensions in chloroform, namely an order of magnitude larger than the solid-state filters of the present study under the same experimental conditions. The discrepancy is worthy if we consider that molecules embedded in a liquid present a strong contribution to the nonlinear refractive index due to molecular reorientation.

The open Z-scan method serves to assess the nonlinear absorption coefficient, β , figure 9 exposes the experimental results. At first sight, as expected, it is noteworthy that the nanoparticle loads greatly enhance the nonlinear absorption behavior. Actually, PMMA/Cr_2O_3 and PMMA/WO_3 optical limiting filters present a broader valley jointly with a significantly deeper drop in transmittance.

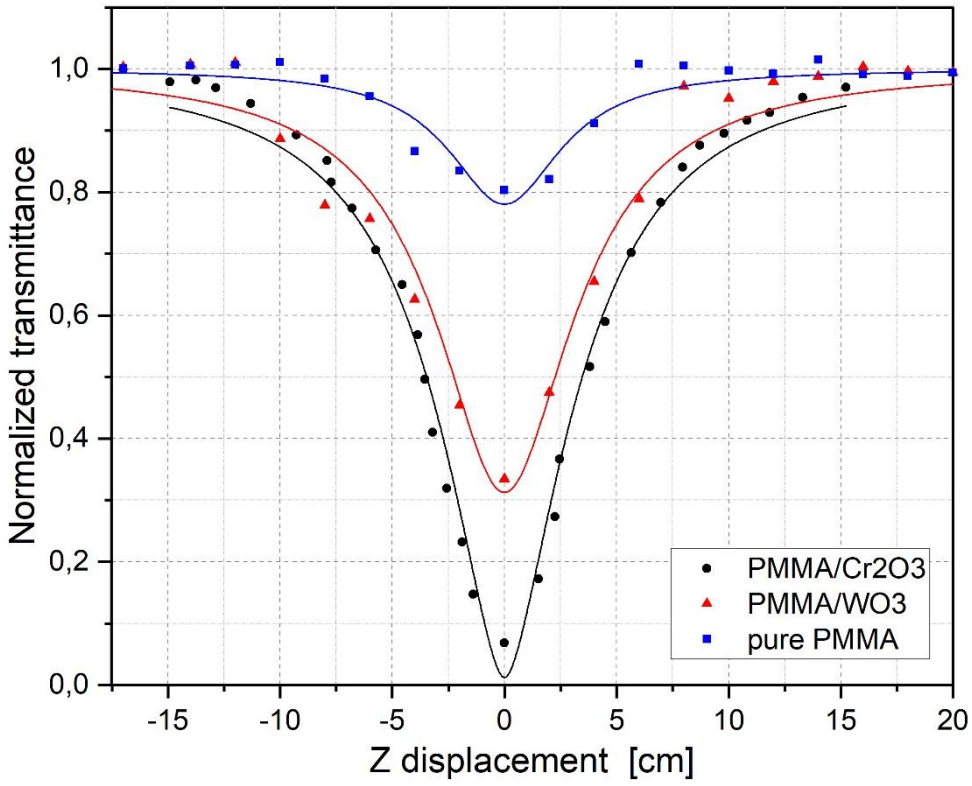

Figure 9: Open Z-scan traces for the PMMA/Cr_2O_3 and PMMA/WO_3 optical limiting filters at an incident laser irradiance $I_0 = 5.10^{10} W / cm^2$ and pure PMMA at an incident laser irradiance $I_0 = 5.10^{11} W / cm^2$. The solid lines denote the theoretical fittings of equation (12). Laser wavelength is 1064 nm.

The values of the nonlinear absorption coefficient β, can be easily deducted from the theory developed in [38] reporting the expression for the open-aperture normalized transmittance in an optical device:

$$T_{norm}(z) = \frac{\ln(1 + q_0(z))}{q_0(z)} \qquad (8).$$

In relation (8), $q_0(z) = \beta I(z) L_{eff}$, stands for the beam parameter that contains β to be assessed and $I(z)$ is the magnitude of the intensity of the Gaussian laser beam travelling in the $+z$ direction. On the propagation axis for $r = 0$, it can be written:

$$I(z) = \frac{I_0 e^{-\gamma}}{1 + a^2} \qquad (9).$$

In equation (9), we consider the extinction of the laser radiation in the propagating medium caused by scattering centers or defects by means of a further parameter γ. Therefore, the substitution in equation (8) brings:

$$T_{norm}(z) = \frac{(1 + a^2)^2}{\beta I_0 L_{eff} e^{-\gamma}} \ln\left(1 + \frac{\beta I_0 L_{eff} e^{-\gamma}}{(1 + a^2)^2}\right) \qquad (10).$$

The nonlinear absorption coefficients β resulting from model fittings according to relation (10) are summarized in table 3. They vary from $1.8\,cm / GW$ to $163\ cm / GW$ for PMMA/WO_3 and PMMA/Cr_2O_3, respectively, while the one for pure PMMA lies 2 orders of magnitude behind. Obviously, the higher value obtained in the case of PMMA/Cr_2O_3 is to be ascribed to RSA enhanced by ESA, whilst the β value calculated for PMMA/WO_3 validates its MPA character. It is to be pointed out that Liao et al. [5], calculated a nonlinear absorption coefficient $\beta = 297\ cm / GW$ in the case of a transition metal based MoS_2/PMMA nanocomposite submitted to nanosecond laser radiations at the wavelength of 532 nm in off-resonant conditions. This value is comparable to the one obtained for the PMMA/Cr_2O_3 nanocomposite. The authors in [5] suggested RSA as the major nonlinear mechanism occurring in their solid-state optical limiting filters which reasonably corroborate our statements on the PMMA/Cr_2O_3 system. One of the previous author's work [20] on the twin systems in the form of suspensions revealed a comparable β value for the PMMA/WO_3 optical filter, whereas a pointedly lower β value was observed for the PMMA/Cr_2O_3 suspension $\beta = 3\,cm / GW$, i.e. factor of 50. This discrepancy might be clarified by the presence of intermolecular charges transfer between the PMMA host molecule and the Cr_2O_3 nanoparticle load which would have the effect of raising the contribution of the nonlinear absorption component.

Table 3: n_2 and β nonlinear parameters of PMMA/Cr_2O_3, PMMA/WO_3 and pure PMMA optical limiting filters at the wavelength of 1064 nm in the nanosecond regime. Further details in the text.

	$n_2\,(cm^2/W)$	$\beta\,(cm/GW)$
PMMA/Cr_2O_3	$-1.6\,X\,10^{-15}$	163
PMMA/WO_3	$-7.1\,X\,10^{-16}$	1.8
pure PMMA	$-2.2\,X\,10^{-17}$	0.02

4. Conclusion

Cr_2O_3 and WO_3 templated nanoparticles were embedded in a PMMA host resulting in efficient optical limiting filters. Optical grade filters with transmittances as high as T=90 % at 1064 nm have been were produced by chemical synthesis from the bulk. To the best of the author's knowledge, the nonlinear optical properties and the optical limiting behavior of Cr_2O_3 and WO_3 embedded in a PMMA matrix at the wavelength of 1064 nm in the nanosecond regime have never been reported. This work showcased the cause routing to optical limiting, more specifically, ESA/RSA in the case of the PMMA/Cr_2O_3 system and MPA for the PMMA/ WO_3 one. The optical limiting performance improvement has been demonstrated for the PMMA/Cr_2O_3 filter bearing out a laser protection level of OD=2.0, a factor of 2 larger than the pure PMMA filter. In that case, 99.99 % of the incoming laser radiations can be filtered out. A significant blue shift in the nonlinear activation threshold energy was observed when WO_3 or Cr_2O_3 are embedded in a PMMA host as the values have been subsequently pulled down from 500 µJ (pure PMMA) to 65 µJ and 23µJ, respectively. Z-scan measurements highlighted a self-defocusing effect as a result of a negative nonlinearity. Nonlinear refractive indexes in the order of $n_2 = -1.0\,X\,10^{-15}\,cm^2/W$ were calculated for the PMMA/Cr_2O_3 and PMMA/ WO_3 systems and $n_2 = -2.2\,X\,10^{-17}\,cm^2/W$ for the pure PMMA. A nonlinear absorption coefficient as high as $\beta = 163\,cm/GW$ has been assessed for the PMMA/Cr_2O_3 optical limiting filter. The ease of manufacture and the level of performance of the PMMA/Cr_2O_3 optical limiting filters make them suitable to be implemented as protection filters in electro optical systems against harmful laser radiations. This research work established consistent ways to promote new performance milestones within the field of laser protection.

5. Acknowledgements

The authors gratefully acknowledge the German Bundesamt für Ausrüstung, Informationstechnik und Nutzung der Bundeswehr (BAAINBw, Germany) and the French Direction Générale de l'Armement (DGA, France) for their financial support.

6. Disclosures

The authors do not declare any financial, personal or professional conflicts of interest.

7. Data availability

The data involved in the results presented in this study are not publicly available at this time but may be obtained from the authors upon request.

8. References

1. O. Muller, C. Hege, M. Guerchoux and L. Merlat, "Synthesis, characterization and nonlinear optical properties of polylactide and PMMA based azophloxine nanocomposites for optical limiting applications", Mater. Sci. Eng. B **276**, 115524 (2022).

2. Qusay M. A. Hassan and R. K. H. Manshad, "Surface morphology and optical limiting properties of azure B doped PMMA film", Opt. Mater. **92**, 22-29 (2019), https://doi.org/10.1016/j.optmat.2019.03.058.
3.] M. Yuksek, E. Ç. Kaya, N. Karabulutlu, A. A. Kaya, M. Karabulutlu and A. Elmali," Enhancing of the nonlinear absorption and optical limiting performances of the phthalocyanine thin films by adding of the single walled carbon nanotubes in poly(methyl methacrylate) host", Opt. Mater. **91**, 326-332 (2019), https://doi.org/10.1016/j.optmat.2019.03.045.
4. F. D'Amore, M. Lanata, S. M. Pietralunga, M. C. Gallazzi and G. Zerbi, "Enhancement of PMMA nonlinear optical properties by means of a quinoid molecule", Opt. Mater. **24**, 661-665 (2004), https://doi.org/10.1016/S0925-3467(03)00181-2.
5. Q. Liao, Q. Zhang, X. Wang, X. Li, G. Deng, Z. Meng, K. Xi and P. Zhan," Facile fabrication of POSS-Modified MoS_2/PMMA nanocomposites with enhanced thermal, mechanical and optical limiting properties", Compos. Sci. Technol. **165**, 388-396 (2018), https://doi.org/10.1016/j.compscitech.2018.07.008.
6. A. Stashans and S. Jácome," Local structure, magnetic and electronic properties of N-doped α-Cr_2O_3 from the first-principles", Comput. Mater. Sci. **81**, 353-357 (2014), https://doi.org/10.1016/j.commatsci.2013.08.042.
7. M. G. Tsegay, H. G. Gebretinsae and Z. Y. Nuru," Structural and optical properties of green synthesized Cr_2O_3 nanoparticles", Materials Today **36** (2), 587-590, (2021), https://doi.org/10.1016/j.matpr.2020.05.503.
8. H. Ekinci, M. Soltani, N. M. S. Jahed, X. Zhu, B. Cui and D. Pushin, "Effect of annealing on the structural, optical and surface properties of chromium oxide (Cr_2O_3) thin films deposited by e-beam evaporation for plasma etching applications",J. Alloys Compd. **875**, 160087 (2021), https://doi.org/10.1016/j.jallcom.2021.160087.
9. N. Kangkun, N. Kiama, N. Saito and C. Ponchio, "Optical properties and photoelectrocatalytic activities improvement of WO_3 thin film fabricated by fixed-potential deposition method", Optik **198**, 163235 (2019), https://doi.org/10.1016/j.ijleo.2019.163235.
10. R. Ponnusamy, R. Venkatesan, R. Samal, M. Kandasamy, V. Gandhiraj and B. Chakraborty, "Bifunctional WO_3 microrods decorated RGO composite as catechol sensor and optical limiter", Appl. Surf. Sci **536**, 147669 (2021), https://doi.org/10.1016/j.apsusc.2020.147669.
11. Z. Y. Wu, L. Cao, P. F. Wu and D.V.L.N. Rao, "Optical nonlinearity and power limiting of nano-sized $BaFe_{12}O_9$ and Cr_2O_3 organosols", Physics of Low-Dimensional Structures **7**, 123-130 (2022).
12. M. Fakhari, M. J. Torkamany and S. N. Mirnia, "Linear and nonlinear optical properties of WO_3 nanoparticles synthesized at different fluences of pulsed Nd:YAG laser", Eur. Phys. J. Appl. Phys. **84**, 30401 (2018), https://doi.org/10.1051/epjap/2018180264.
13. M.S. Brodyn, S.A. Mulenko, V.I. Rudenko, V.R. Lyakhovetskyi, M.V. Volovyk and N. Stefan, "Cubic Optical Nonlinearity of Thin Fe_2O_3 and Cr_2O_3 Films Synthesized by Pulsed Laser Deposition", Ukr. J. Phys. **61** (6), (2016), https://doi.org/10.15407/ujpe61.06.0495 .
14. Z. T. Khodair, G. A. Kazem and A. A. Habeeb, "Studying the optical properties of (Cr_2O_3:I) thin films prepared by spray pyrolysis technique", Iraq. J. Phys. **10**, 83-89 (2012).
15. Y. Tanabe, M. Muto and E. Hanamura, "Theory of nonlinear optical susceptibility of antiferromagnetic Cr_2O_3", Solid State Commun. **102** (9), 643-646 (1997).
16. F. Bussolotti, L. Lozzi, M. Passacantando, S. La Rosa, S. Santucci and L. Ottaviano, "Surface electronic properties of polycrystalline WO_3 thin films: a study by core level and valence band photoemission", Surf. Sci. **538**, 113-123 (2003).
17. X. Liu and H-Q. Fan, "Electronic structure, elasticity, Debye temperature and anisotropy of cubic WO_3 from first-principles calculation", R. Soc. Open Sci. **5**, 171921 (2018), http://dx.doi.org/10.1098/rsos.171921.
18. K. Balamurugan, S. Mandal, N. H. Kumar and P. N. Santhosh," Magnetic and optical properties of Cr_2O_3 nanoparticles", Proc. of the DAE Solid State Physics Symposium **51**, 365-366 (2007).
19. J. Zhu, M. Vasilopoulou, D. Davazoglou, S. Kennou, A. Chroneos and U. Schwingenschlögl, "Intrinsic Defects and H Doping in WO_3", Sci. Rep. **7**, 40882 (2017).
20. O. Muller and P. Gibot, "Optical limiting properties of templated Cr_2O_3 and WO_3 nanoparticles", Opt. Mater. **95**, 109220 (2019).
21. www.militaryaerospace.com/articles/2014/06/elbit-observation-laser.html.
22. www.militaryaerospace.com/articles/2014/03/northrop-laser-designator.html.
23. P. Gibot and L. Vidal, "Original synthesis of chromium (III) oxide nanoparticles", J. Eur. Ceram. Soc. **30**, 911-915 (2010).
24. P. Gibot, M. Comet, L. Vidal, F. Moitrier, F. Lacroix, Y. Suma, F. Schnell and D. Spitzer, "Synthesis of WO_3 Nanoparticles for Superthermites by the Template Method from Silica Spheres", Solid State Sci. **13**, 908-914 (2011).
25. P. Zhan, J. Chen, A. Zheng, H. Shi, F. Chen, D. Wei, X. Xu and Y. Guan, " The Trommsdorff effect under shear and bulk polymerization of methyl methacrylate via reactive extrusion", Eur. Polym. J. **122**, 109272 (2020), https://doi.org/10.1016/j.eurpolymj.2019.109272.
26. S. Liang, H. l. Zhang, M. Luo, K. Luo, P. Li, H. Xu and Y. Zhang, "Colour performance investigation of a Cr_2O_3 green pigment prepared via the thermal decomposition of CrOOH", Ceram. Int. **40**, 4367-4373 (2014).
27. R. Sivakumar, R. Gopalakrishnan, M. Jayachandran and C. Sanjeeviraja, "Preparation and characterization of electron beam evaporated WO_3 thin films", Opt. Mater. **29**, 679-687 (2007).

28. T. Altalhi, A. A. Gobouri, M. S. Refat, M. M. El-Nahass, A.M. Hassanien, A. A. Atta, S. Al Otaibi and A.M. Kamal, "Optical spectroscopic studies on poly(methyl methacrylate) doped by charge transfer complex", Opt. Mater. **117**, 111152 (2021).
29. R. I. Jasim, M. A. Jabbar and A. N. Jameel, "Effect of doping on energy gap of PMMA/ Cr_2O_3 blend Films", Int. J. Adv. Sci. Res. **2** (5), 01-05, ISSN: 2456-0421 (2017).
30. S. B. Aziz, O. G. Abdullah, A. M. Hussein and H. M. Ahmed, "From Insulating PMMA Polymer to Conjugated Double Bond Behavior: Green Chemistry as a Novel Approach to Fabricate Small Band Gap Polymers", Polym. **9** (11), 626-15 (2017), https://doi.org/10.3390/polym9110626.
31. W. Matysiak, T. Tanski, P. Jarka, M. Nowak, M. Kepinska and P. Szperlich, "Comparison of optical properties of PAN/TiO_2, PAN/Bi_2O_3, and PAN/SbSI nanofibers", Opt. Mater. **83**, 145-151 (2018).
32. M. M. Abdullah, F. M. Rajab and S. M. Al-Abbas, "Structural and optical characterization of Cr_2O_3 nanostructures: Evaluation of its dielectric properties", AIP Adv. **4**, 027121 (2014).
33. S. J. Varma, J. Kumar, Y. Liu, K. Layne, J. Wu, C. Liang, Y. Nakanishi, A. Aliyan, W. Yang, P. M. Ajayan and J. Thomas, "2D TiS_2 Layers: A Superior Nonlinear Optical Limiting Material", Adv. Opt. Mater. **5** (24), 1700713 (2017), https://doi.org/10.1002/adom.201700713.
34. A. Sharma, P. Khan, D. Mandal, M. Pathak, C. S. Rout and K. V. Adarsh, "Unveiling and engineering of third-order optical nonlinearities in $NiCo_2O_4$ nanoflowers", Opt. Let. **46** (23), 5930-5933 (2021).
35. A. Sharma, P. Khan, M. Pathak, C. S. Rout and K. V. Adarsh, "Nonlinear Optical Limiting with Hybrid Nanostructures of $NiCo_2O_4$ and Multiwall Carbon Nanotubes", (Preprint) arXiv: 2204.04751 (2022),https://doi.org/10.48550/arXiv.2204.04751 .
36. T. Larbi, B. Ouni, A. Gantassi, K. Doll, M. Amlouk and T. Manoubi, "Structural, optical and vibrational properties of Cr_2O_3 with ferromagnetic and antiferromagnetic order: A combined experimental and density functional theory study ", J. Magn. Mater. **444**, 16-22 (2017).
37. M. Sheik-Bahae, A. A. Said, T. H. Wei, D. J. Hagan and E. W. Van Stryland, "Sensitive Measurement of Optical Nonlinearities using a Single Beam", IEEE J. Quantum Electron. **26**, 760-769 (1990).
38. R. A. Ganeev, A. I. Ryasnyansky, S. R. Kamalov, M. K. Kodirov and T. Usmanov, "Nonlinear susceptibilities, absorption coefficients and refractive indices of colloidal metals ", J. Phys. D **34**, 1602-1611 (2001).